Biosensors and Bioelectronics 159 (2020) 112187

Contents lists available at ScienceDirect

Biosensors and Bioelectronics

journal homepage: http://www.elsevier.com/locate/bios

# Multiplex label-free biosensor for detection of autoantibodies in human serum: Tool for new kinetics-based diagnostics of autoimmune diseases

A.V. Orlov [a,b,*,1], A.V. Pushkarev [a,b,1], S.L. Znoyko [a], D.O. Novichikhin [a,c], V.A. Bragina [a], B. G. Gorshkov [a], P.I. Nikitin [a,c]

[a] Prokhorov General Physics Institute of the Russian Academy of Sciences, 38 Vavilov St, 119991, Moscow, Russia
[b] Moscow Institute of Physics and Technology (National Research University), 9 Institutskii per., Dolgoprudny, Moscow Region, 141700, Russia
[c] National Research Nuclear University MEPhI (Moscow Engineering Physics Institute), 31 Kashirskoe shosse, 115409, Moscow, Russia

ARTICLE INFO

*Keywords:*
Label-free biosensing
Diagnostics of autoimmune diseases
Autoantibody activity
Surface-induced conformational changes
Human serum

ABSTRACT

A multiplex label-free biosensor is developed for diagnostics of autoimmune diseases by highly sensitive measuring in human serum both critical characteristics of autoantibody: concentration and native kinetic parameters that reflect autoantibody aggressiveness to the organism's tissues. The biosensor is based on the spectral-correlation interferometry and image processing of a microarray glass biochip, affordable to be single-used in medical applications. Simultaneous 25-min detection and activity characterization of several autoantibodies in the same serum sample have been demonstrated for anti-thyroglobulin (anti-TG) and anti-thyroid peroxidase (anti-TPO) as models. The biosensor offers extremely high sensitivity: limits of detection in serum are 1.7 IU/mL and 6 IU/mL for anti-TPO and anti-TG, respectively. The dynamic range covers the whole range of clinically relevant concentrations of the autoantibodies up to 1000 IU/mL. The developed method of characterization of autoantibody activity by recording the kinetics of their binding with free native antigens is based on autoantibody polyvalency. The measurements in clinical serum samples have shown that the native kinetic parameters are independent of concentration. The proposed biosensor and method of native kinetic registration can be used to develop new criteria for comprehensive diagnostics of autoimmune diseases, based not only on traditional measurements of concentration but also on quantitative evaluation of autoantibody aggressiveness. The developed method can be adapted to other label-free sensors such as those based on the surface plasmon resonance, optical waveguides, etc.

## 1. Introduction

Autoantibodies are associated with more than 80 serious autoimmune disorders of enormous economic impact, exceeding that of cancer (Conigliaro et al., 2016; Krumbholz et al., 2012; Rose, 2008; ASCIA, 2013). These entities can serve not only as predictors of autoimmune disorders long before the clinical onset but also as markers of disease activity and severity (Damoiseaux et al., 2015; Nesterova et al., 2006; Wu et al., 2017; Zhang and Zhao, 2018).

Unlike usual antibodies that fight a disease, autoantibodies target the organism's own tissues (Lleo et al., 2010; Marrack et al., 2001; Scofield, 2004). Therefore, for diagnosing an autoimmune disorder, it is necessary to determine in serum not only concentration of autoantibodies but also their destructive potential with respect to the tissues (Božič et al., 2005; Cui and Zhao, 2005; Thaler et al., 2009). The latter parameter can be estimated by measuring the kinetics of autoantibody binding with free, non-immobilized antigens that present native conformation.

The dramatic difference in the results of various commercial methods for measuring autoantibody is rather common. As an example, the median concentrations of frequently assessed autoantibodies such as anti-thyroglobulin and anti-thyroid peroxidase determined by test systems of different manufacturers for the same group of patients may vary from 0.53 to 14.23 IU/mL for the former (D'Aurizio et al., 2017), and from 0.2 to 10.0 IU/mL for the latter (Tozzoli et al., 2017). The most likely cause is kinetic heterogeneity of autoantibodies in real samples (Amos and Bridges, 2005). Another possible reason is different labels used in many techniques, e.g., enzyme-linked immunosorbent assays (ELISA), electrochemiluminescent immunoassays (ECLIA), etc.

* Corresponding author. Prokhorov General Physics Institute of the Russian Academy of Sciences, 38 Vavilov St, 119991, Moscow, Russia.
*E-mail address:* alexey.orlov@kapella.gpi.ru (A.V. Orlov).
[1] These authors contributed equally to this work.

https://doi.org/10.1016/j.bios.2020.112187
Received 30 November 2019; Received in revised form 29 March 2020; Accepted 2 April 2020
Available online 11 April 2020

(Campuzano et al., 2019; Houen, 2019; Mahler et al., 2016; Sciascia and Bertolaccini, 2016). The labels may destroy the binding sites that participate in antibody-antigen interactions, on the one hand, and non-specifically interact with proteins immobilized on a surface, on the other hand (Cooper, 2009; Fan et al., 2008; Orlov et al., 2018; Seydack, 2005).

The label-free techniques are not prone to the label-associated issues. These techniques generally offer shorter assay times because of excluding the labelling step, and more importantly, due to avoidance of any further reaction (e.g. enzymatic) for indirect detection of target. Real-time monitoring of biomolecular interactions is another advantage. Traditional label-free biosensors, e.g., those based on the surface plasmon resonance (SPR) (Ayela et al., 2007; Campbell and Kim, 2007), nanotube-based sensors (Drouvalakis et al., 2008), photonic ring immunoassay (Mudumba et al., 2017), and many others usually register autoantibody interactions with antigen immobilized on a sensor surface. Therefore, their results on binding kinetics may differ from native kinetics due to unpredictable conformation of the surface-deposited antigens, which may conceal some epitopes from antibody binding. Besides, the biochips for commercial label-free biosensors that dominate on the market, e.g., quartz microbalance sensors (Anderson et al., 2007; Qiao et al., 2016; Su et al., 2005) and SPR based on precisely deposited gold films (Mauriz et al., 2016; Scarano et al., 2010), are too expensive to be single-used. At the same time, the biochip regeneration can hardly be considered for practical medical diagnostics.

The label-free biosensing techniques capable of determining in blood not only concentration but also native kinetics of autoantibody using affordable disposable biochips are still to be developed for biomedical applications.

Here, we present a highly sensitive multiplex biosensor that permits rapid (25 min) and simultaneous label-free measuring in human blood serum of both critical characteristics of autoantibody: i) concentration and ii) native kinetic parameters that indicate the antibody aggressiveness toward the organism's tissues. These parameters are promising for development of more accurate criteria for early diagnostics and efficient therapy of autoimmune disorders. As clinically relevant models, anti-thyroid peroxidase (anti-TPO) and anti-thyroglobulin (anti-TG) were selected. They are present in 90–95% and 70–80%, respectively, of patients with autoimmune thyroid diseases (Fröhlich and Wahl, 2017). The simultaneous detection of these autoantibodies is important for differential diagnostics of thyroid diseases. In patients with Hashimoto thyroiditis, for example, both anti-TPO and anti-TG are elevated. An increased level of only one of these autoantibodies may be indicative of other disorders, namely: at the higher anti-TPO – Graves' disease, while at anti-TG – thyroid hypertrophy or small nodules (Martinez and Prabhakar, 2006).

The analytical characteristics of the biosensor surpass those of the majority of label-based techniques: the detection limits in serum are 1.7 IU/mL and 6 IU/mL for anti-TG and anti-TPO, respectively. The dynamic range covers the whole range of clinically relevant concentrations up to 1000 IU/mL. To the best of our knowledge, this is the first label-free biosensor capable of measuring the kinetic parameters of autoantibody interaction with free antigen in the form as it presents in blood, not being immobilized on a surface. The developed approach overcomes the bottleneck of label-free biosensing – high non-specific binding in human blood serum. This factor does not affect the signal of our biosensor. That is an especially useful feature for autoantibodies as they should be studied directly in serum (blood) of the organism where they are produced. The biosensor is based on the reflectometric principle of spectral correlation interferometry (SCI) (Nikitin et al., 2003). The SCI offers real-time measuring in metrological units of changes in optical thickness of the biolayer on a biochip surface due to biochemical reactions. Importantly for medical applications, SCI permits using microscope cover glass slips as single-used biochips compatible with the glass microarray format. Unlike refractometric label-free techniques, e.g., SPR-based ones, SCI is insensitive to bulk refractive index of analyzed solutions. The presented biosensor is promising for high-throughput microarray-based differential diagnostics of autoimmune diseases.

## 2. Experimental

### 2.1. Reagents

The following reagents were used in this study: bovine serum albumin (BSA), (3-Aminopropyl)triethoxysilane (APTES), N-(3-Dimethylaminopropyl)-N-ethylcarbodiimide hydrochloride (EDC), phosphate buffered saline (PBS), succinic anhydride, glycine, tetramethylbenzidine, Tween-20 (Sigma Aldrich, USA); 2-(N-morpholino) ethanesulfonic acid (MES) (AppliChem, Germany); horseradish peroxidase conjugated with goat antihuman immunoglobulin G (Abcam, USA); sulphuric acid, methanol, dimethylformamide (Chimmed, Russia); thyreoperoxidase, thyroglobulin, goat monoclonal antibodies against human IgG (Xema medica, Russia; GeneTex, USA; Russian Research Center for Molecular Diagnostics and Therapy, Russia); serum standards and samples from patients (Russian Cardiology Research and Production Complex of Russian Ministry of Health, Russia). Ethical approval for this study was obtained from the ethics committee of the Russian Cardiology Research and Production Complex of Russian Ministry of Health (approval No. 247).

### 2.2. Multiplex label-free biosensor

The multiplex label-free biosensor employs radiation from a broadband superluminescent diode (SLD-381-MP, Superlum Diodes, Ltd., Russia) in an optical SCI-scheme that comprises two interferometers (Nikitin et al., 2003, 2005). The base (inter-mirror distance) of one Fabry–Perot interferometer is periodically changed with a piezoelectric driver. A microscope glass cover slip serves simultaneously as a biochip and the second two-beam reflective interferometer. During biochemical reactions on the biochip, the optical thickness of the slip with the bound biological layer changes. To measure such changes, the interference between a reference beam reflected from the bottom surface of the slip and a beam reflected from the "biolayer – analyzed sample" interface is used. Variations in optical thickness of the biomolecule layer on the recognition spots on the biochip are calculated by phase changes of correlation signals from a 12-bit monochrome CCD-camera (Basler, Germany). For simultaneous registration of biochemical reactions in several recognition spots, their image signals are averaged over the area of each recognition spot. The SCI principle was verified by various independent techniques and applied studies (Ivanov et al., 2011; Burenin et al., 2015; Znoyko et al., 2018; Orlov et al., 2018).

The multiplex microarray biosensor designed for this research recorded in real time sensograms as temporal dependences of the biolayer thickness changes in separate recognition spots. Each stage of the experiments was considered completed when the sensograms plateaued. PBS buffer was passed for washing between the stages.

### 2.3. Preparation of biochips

First, the biochip surface was carboxilated for efficient and rapid immobilization of biomolecules (Hermanson, 2013; Ngunjiri et al., 2013; Rusmini et al., 2007). For this purpose, the thoroughly cleaned microscope cover slips were incubated for 16 h under an exhaust hood in 3% solution of APTES in methanol and then for 2 h in 15 mM solution of succinic anhydride in dimethylformamide. Then the slips were thermally processed in a dry heat oven at 105 °C for 1 h with further washing at room temperature. The chips were activated by 15-min incubation in 20 mg/mL solution of EDC in MES (0.1 M, pH 5.0). Then 50 μg/mL of antigens in PBS (pH 7.4) was deposited in different sensing spots at room temperature to achieve covalent immobilization of antigen onto the biochip due to interaction of antigen amino groups with the activated carboxyl groups on the surface. The antigen deposition was carried out

in the liquid handling system of the biosensor for 15 min at the flow rate of 6.7 μL/min. All stages of the biochip preparation (Figure 13 in the related Data in Brief article) were controlled with the X-ray photoelectron spectroscopy (XPS). The XPS-spectra along with the description of antigen attachment mechanism can be found in section 7 of the related Data in Brief article. Besides, we have established that the stable immobilization of proteins on the fabricated surface can be achieved only after its activation with carbodiimide (related Data in Brief article, Figure 15). The surface was blocked with a mixture of 1% glycine and 0.5% of BSA in PBS buffer. The prepared biochips can be stored without deterioration for a long time until using (Data in Brief article, Figure 16).

### 2.4. Measuring procedure

All experiments in this research were carried out in human blood serum. Each of the samples contained various amounts of anti-TG and anti-TPO, naturally produced by the immune system of the patients (not spiked). 50 μL of the human blood serum was diluted with 40 μL of 10 mg/mL of PBS-BSA and then pumped for 10 min at room temperature along the glass biochip having respective antigens pre-immobilized in different sensing spots. The kinetic constants of autoantibody interaction with native antigen were calculated using the sensograms obtained in these experiments and the model described in section 1 of the related Data in Brief article. The biolayer increment at the latter step was measured as the signal, which was free of non-specific contributions. For determination of autoantibody concentration in human serum, a solution of secondary recognition antibody (goat antibody to human immunoglobulins) at 50 μg/mL in PBS was pumped.

### 2.5. Independent verification with enzyme-linked immunosorbed assay (ELISA)

Antigen solution (TPO or TG) was added to the wells of a microtiter plate at a concentration of 50 μg/mL and incubated during 4 h at room temperature. Then, the wells' surface was blocked by 2-h incubation with the solution of 5% BSA in PBS. Next, 100-μL serum samples were added and incubated for 2 h. After that, incubation with horseradish peroxidase conjugated with antihuman immunoglobulin G was implemented followed by addition of tetramethylbenzidine solution and measuring the absorbance in each well at 450 nm. Triple washing of the wells with PBS with 0.1% Tween-20 was done in between the mentioned stages.

### 2.6. Data processing

All the experiments were carried out at least three times. In graphs, each value represents a mean, and error bars show standard deviations. The calibration curves were approximated by the log-log linear regression. The limit of detection was calculated using both 2σ and 3σ criteria as the minimal concentration, at which the signal exceeded that of a negative control by at least two and three standard deviations, respectively (Chaloner-Larsson et al., 1999; Thomsen et al., 2003).

## 3. Results and discussion

### 3.1. Setup for microarray biosensing

The advantage of SCI registration technique is the capability of multiplex operation for independent and simultaneous label-free measuring of several analytes using a single-used multi-spot glass biochip. The registration principle is shown in Fig. 1. Antigens (here, TPO or TG) are covalently pre-immobilized at different spots on the biochip. The analyzed sample is pumped along the surface. The biolayer thickness variations caused by intermolecular binding is registered by a CCD-detector for each spot independently. The correlation signal of two interferometers, including the scanned Fabry–Perot interferometer, is analyzed (see details in Experimental, section 2.2).

Although the results discussed below were obtained in the multiplex mode, the plots for different analytes are shown separately for the sake of clarity.

### 3.2. Determination of native kinetics of autoantibodies in clinical samples

The approach to assessment of autoantibody aggressiveness to the organism's tissues by measuring kinetic characteristics of autoantibody binding with native, non-immobilized antigen is based on autoantibody polyvalency. The registration scheme, which does not involve labels, and characteristic sensograms recorded in real time are shown in Fig. 2. The measuring procedure consisted of two major steps. First, we pumped the analyzed serum sample along the biochip with immobilized capture antigens. At the second step, a solution containing native antigens was passed.

Fig. 2 illustrates the method operation on the example of autoantibodies of IgG class. Since these molecules possess two antigen binding fragments (Fab), some autoantibodies may have only one fragment bound to an antigen at the first step. Then the other Fab fragment is capable of binding the native antigen from the sample pumped during the second step. This way, we directly register interactions between the autoantibody, which has a free Fab fragment, and a non-immobilized antigen as it presents in blood. The scheme functions similarly in the presence in serum of IgM that has ten Fab-fragments because if such a molecule is sorbed on the surface at the first step, it retains the ability of binding to antigen at the second step. This approach for the first time permits real-time registration of the kinetics of autoantibody binding with native antigen and determination of kinetic constants of their interaction. Importantly, while this method registers non-specific

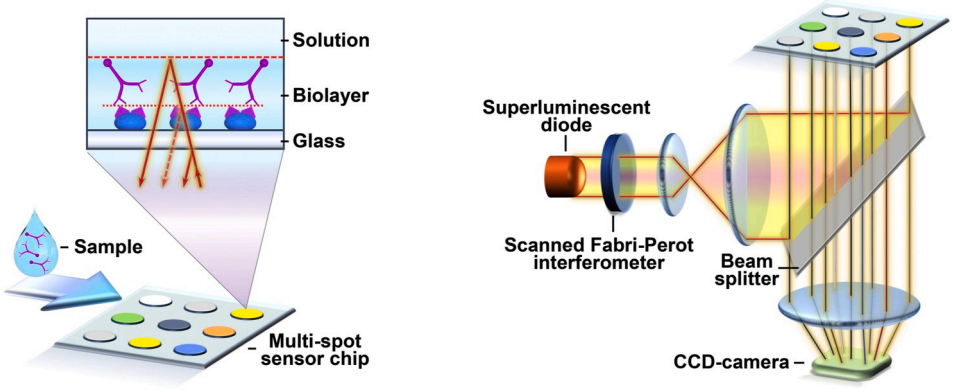


**Fig. 1.** Principle of multiplex measurements with multi-spot glass biochip (*left*) and optical scheme of the biosensor based on imaging spectral-correlation interferometry for diagnostics of autoimmune diseases (*right*).

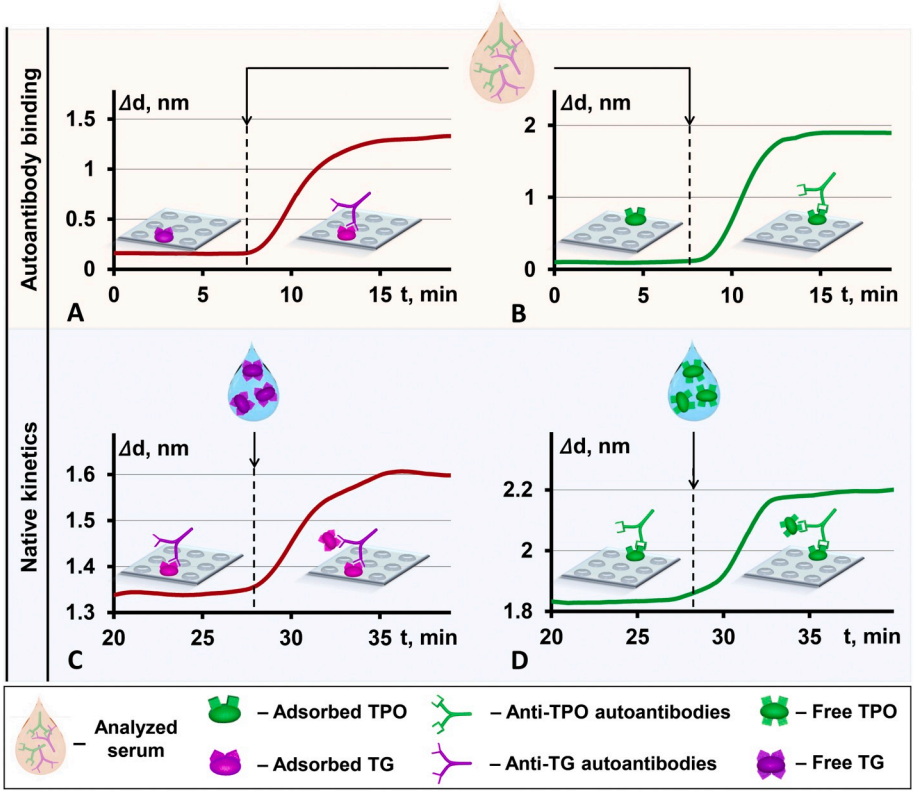


**Fig. 2.** Schemes and experimental sensograms for simultaneous measuring the kinetics of interaction of anti-thyroglobulin and anti-thyroid peroxidase IgG autoantibodies with non-sorbed target antigens: first step (*top row*) – binding of serum autoantibodies with immobilized TG (A) and TPO antigens (B) via one antigen binding fragment; second step (*low row*) – determination of native kinetics by recording the interaction of free thyroglobulin (C) and free thyroid peroxidase (D) with the other antigen binding fragments of the autoantibodies.

binding of serum components during the first step, it is interaction of autoantibody with native antigen that is recorded at the second step.

Hypothetically, some autoantibodies may suffer from steric hindrance for antigen binding due to close contact of the second Fab fragment with the surface. With a large number of autoantibodies bound by the antigen immobilized onto the surface, the kinetic constant of association ($k_{on}$) might potentially decrease because of the steric effect. To verify the absence of the steric effect influence, the kinetic constants were compared for the same serum in three variants: undiluted, and diluted 3-fold, and 9-fold. This way, the serum samples had different concentrations of autoantibodies. The concentration of undiluted serum was close to the upper limit of clinically relevant range – 864 IU/mL of anti-TPO. The determined kinetic constant was the same within the experimental error (see Table 1 in the related Data in Brief article). These results indicate no significant influence of the steric effect on the kinetic constant, which does not depend on autoantibody concentration. That is probably because in the clinically relevant range of concentrations, the antibodies seem to occupy rather small fraction of the surface and are sufficiently spaced apart not to interfere.

The kinetic characteristics of binding of native antigen with anti-TPO and anti-TG antibodies were measured in human clinical samples of eight patients (Table 1). It can be seen that the values of kinetic constant of association, which determine the rate of antigen binding, significantly vary in different patients, in particular, by 9.2 and 12.5 times for anti-TPO and anti-TG, respectively. At the same time, the kinetic data do not reveal any correlation with autoantibody concentration. One may find quite different combinations in Table 1. While serum samples #1 and #2 exhibit relatively low anti-TG autoantibody concentration, the kinetic constant for the former is fairly low, but for the latter, on the contrary, features the highest kinetic constant. Apparently, the kinetic characteristics of autoantibodies are concentration-independent parameters (the coefficients of correlation $R^2$ between kinetic characteristics and autoantibody concentration equal 0.08 and 0.04 for anti-TPO and anti-TG, respectively).

Notably, one of the reasons of the incompatible reference ranges of various traditional tests for anti-TPO and anti-TG by different manufacturers is kinetic heterogeneity of antibodies in real samples (D'Aurizio et al., 2017; Tozzoli et al., 2017). Another reason is that the majority of platforms register interactions of the analyzed autoantibody with antigen sorbed on a solid phase, which may cause the antigen to present its different sites depending on the sorption method (Danczyk et al., 2003; Ivanov et al., 2019; Makaraviciute and Ramanaviciene, 2013). Therefore, the serum samples, which have the same autoantibody concentration but different kinetics of antigen binding or profile of antigen-binding sites, may yield different results depending on such conditions as incubation time, sensing format, method of antigen sorption and conformation changes due to sorption.

**Table 1**
Kinetic characteristics of native antigen binding with autoantibodies in clinical samples. Values represent means ± standard deviations, n = 3.

| Patient # | Anti-thyroid peroxidase autoantibody | | Anti-thyroglobulin autoantibody | |
|---|---|---|---|---|
| | [C], IU/mL | $k_{on} \times 10^6$, $IU^{-1} \times s^{-1} \times mL$ | [C], IU/mL | $k_{on} \times 10^6$, $IU^{-1} \times s^{-1} \times mL$ |
| **1** | 0.9 | 10.2 ± 1.3 | 5.8 | 28.0 ± 9.9 |
| **2** | 865 | 93.5 ± 16.8 | 73 | 98.8 ± 22.4 |
| **3** | 1.1 | 36.0 ± 7.2 | 212 | 20.8 ± 2.5 |
| **4** | 0.8 | 79.7 ± 10.3 | 384 | 36.0 ± 9.6 |
| **5** | 2.4 | 18.4 ± 1.6 | 507 | 7.9 ± 1.6 |
| **6** | 33.9 | 41.7 ± 10.4 | 162 | 22.3 ± 3.3 |
| **7** | 109 | 95.7 ± 16.3 | 334 | 74.3 ± 17.8 |
| **8** | 785 | 30.4 ± 6.4 | 407 | 63.7 ± 12.7 |

The specificity of the developed label-free biosensor for registration of native kinetics was confirmed by the fact that the signal did not depend upon presence in the sample of non-target molecules, e.g., other low- and high-molecular weight substances (see details in the related Data in Brief article, subsection 2.5).

In addition, no detectable signal was recorded in the control

experiments (Figure 6 of the related Data in Brief article), in which the serum sample without spiked antigen was passed. This way, we verified that a certain part of autoantibodies from the patients' serum actually bound with antigens on the surface via only one of the two "arms", and the response produced by further passing of the free antigen corresponded to the native kinetics.

### 3.3. Detection of autoantibody concentration in human serum

The proposed multiplex biosensor can be also used for rapid, simultaneous and independent measurements of concentration of different autoantibodies in human serum using the affordable single-used biochips. The measuring principle and a characteristic sensograms recorded in real time during the experiments are shown in Fig. 3.

At the final step, secondary anti-human antibodies are pumped to detect specifically the autoantibodies bound in the respective recognition spots of the biochip. The biolayer increment at the final step is considered as the detectible signal.

The signal here is caused solely by the presence of analyzed autoantibodies and does not depend upon unpredictable non-specific binding of serum components with the biochip surface. The specificity of the developed label-free biosensor was confirmed in the experiments with a wide variety of potentially interfering molecules (see details in section 2 in the related Data in Brief article). Another series of experiments was devoted to the study of interference between the immobilized protein array (see details in subsection 2.4 of the related Data in Brief article). It was found in both cases that the non-target molecules did not produce any noticeable effect on the signal within experimental error. The principle is versatile because the same solutions are pumped over the whole surface of the biochip during all steps regardless of the number and specificity of analyzed autoantibodies.

### 3.4. Analytical characteristics of the multiplex sensing

Such parameters as type of the biochip surface, duration of each sensing step, reagent proportions, flow rate, pH, etc. were optimized to maximize the signal and minimize non-specific binding in human serum (for details, see section 3 in the related Data in Brief article). Briefly, the following conditions were selected as optimal: glass modification – carboxylation; flow rate – 6.7 μL/min; pH – 7.4; duration of secondary antibody pumping – 6 min; duration of pumping at other steps – 15 min. Under the optimized conditions, anti-TPO and anti-TG autoantibodies were simultaneously measured in human blood serum. The calibration plot for anti-TPO autoantibody (Fig. 4A) was measured with the calibrated samples of 2.5, 5, 10, 20, 50, 200 and 860 IU/mL. The respective dependence for anti-TG autoantibody (Fig. 4B) was obtained with the calibrated serum samples containing concentrations of 5, 10, 20, 40, 100, 200, 400 IU/mL.

The obtained calibration data are well fitted by a linear log-log relationship with the correlation coefficient of $R^2 > 0.98$ for both anti-TPO and anti-TG. That is fully consistent with the Freundlich adsorption model, which, unlike the Temkin or standard Langmuir models, describes adsorption on heterogeneous surfaces under non-linear distribution of active sites and their energies (Foo and Hameed, 2010). The autoantibodies from patient serum are kinetically heterogeneous so the description of their interaction with a homogeneous surface is mathematically equivalent to the description of interaction of kinetically homogeneous adsorbates with heterogeneous surface considered in Freundlich model.

Additionally, the Freundlich model allows one to determine the heterogeneity index using the slope k of the log-log calibration plot. The steeper the slope, the lower heterogeneity index, and at $k = 1.0$ the model corresponds to the standard homogeneous Langmuir model in the low concentration range. Our experiments show that anti-thyroid peroxidase autoantibody ($k = 0.33$) is considerably more kinetically heterogeneous than anti-thyroglobulin autoantibody ($k = 0.83$).

The limits of detection determined using the 2σ and 3σ criteria are shown in Table 2 along with the dynamic ranges. These analytical characteristics provide reliable detection of both model autoantibodies within the whole range of clinically relevant concentrations, which are also given in this table.

The biosensor performance was validated by correlation with ELISA. The obtained data (Figure 11 and Table 4 of the related Data in Brief article) show high correlation ($R^2 = 0.9506$) between the results obtained with both methods during detection of anti-TG for five clinical samples of serum. Such good correlation is, most likely, due to the same reagents used in both cases. Meanwhile, the developed label-free multiplex biosensor offers 5 times better LOD (for ELISA, the achieved LODs are 8 and 25 IU/mL for anti-TPO and anti-TG, respectively) and about an order better linear dynamic range.

The developed biosensor features high selectivity. As can be seen in Table 4 of the related Data in Brief article, the tested serum samples contain different combinations of the target analytes, namely: the samples of patients #2 and #3 have relatively high concentrations of anti-TG and more than 100-fold difference in anti-TPO; the samples of patients #1 and #5 contain small amounts of anti-TPO but substantially differ in anti-TG concentrations. However, the results for each analyte measured by the developed biosensor reliably correlate with those obtained with ELISA, regardless of concentration of the other analyte. Besides, the good accuracy of the biosensor was confirmed in dilution and recovery experiments (see details in the related Data in Brief article, section 6).

The demonstrated analytical characteristics are better than those of SPR-based label-free methods (Carlsson et al., 2008) and on par with the most sensitive chemiluminescence-based techniques (D'Aurizio et al., 2017; Tozzoli et al., 2017). For side-by-side comparison, see the related Data in Brief article, Table 5. The rarely used nowadays radioimmunoassay-based methods, which remain the most reliable

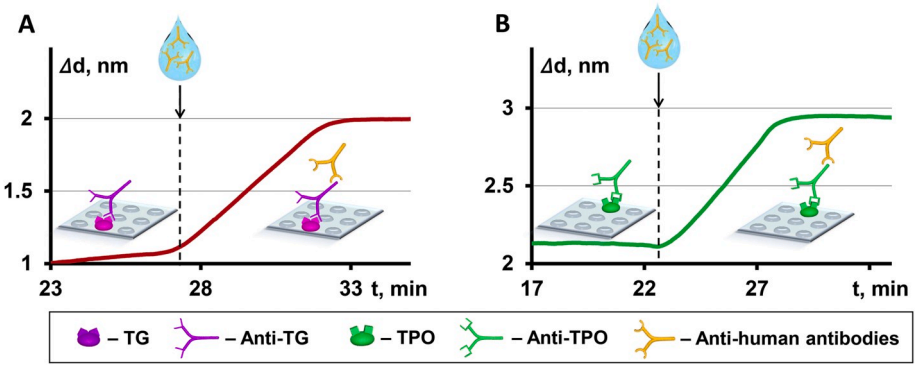


**Fig. 3.** Scheme of detection of autoantibody concentration in human serum and experimental sensograms that represent simultaneous detection of anti-TG (A) and anti-TPO (B) autoantibodies in human serum in different spots of glass biochip.

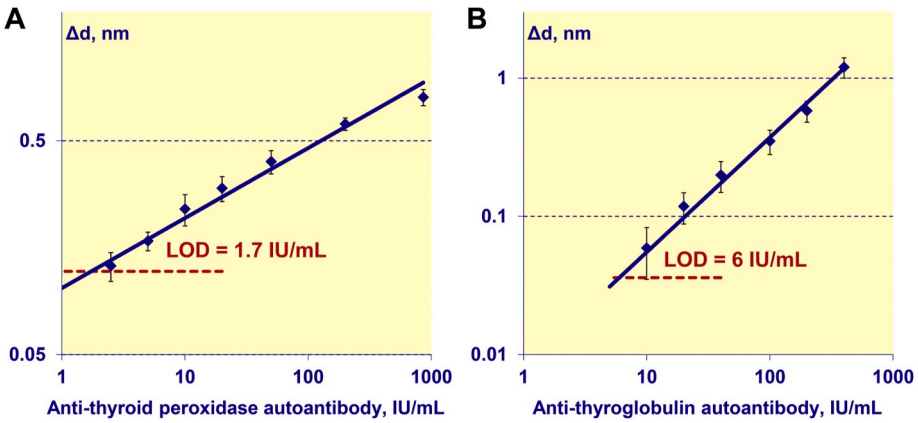


**Fig. 4.** Calibration plots as dependences of biolayer thickness changes upon anti-TPO (A) and anti-TG (B) concentration at the stage of passing of anti-human antibody.

**Table 2**
Analytical characteristics of the developed multiplex biosensor.

| Analyte | Autoantibodies to thyroid peroxidase | | Autoantibodies to thyroglobulin | |
|---|---|---|---|---|
| Parameter | Value recorded | Value in health | Value recorded | Value in health |
| Limit of detection by 2σ/3σ criteria | 1.7/2.5 IU/mL | <3–35 IU/mL[a] | 6/9 IU/mL | <7–115 IU/mL[a] |
| Dynamic range | 1.7–860 IU/mL | | 6–400 IU/mL | |

[a] reference values dependent on region and used method (D'Aurizio et al., 2017; Tozzoli et al., 2016).

among the label-based methods due to the smallest, atom-sized labels, can register anti-TPO and anti-TG on the level of 2 IU/mL and 13 IU/mL, respectively, at the dynamic ranges comparable with those of ELISA methods (isotop.hu, 2019a, 2019b). However, the mentioned traditional techniques are time- and labor-consuming. In contrast, the biosensor designed and tested here is rapid (<25 min), uses affordable and widely available consumables, permits real-time monitoring of all sensing stages and allows multiplexing. It should be noted that the developed biosensing procedure is identical for diverse autoantibodies in a single sample; it differs solely by antigens deposited in the recognition spots.

Remarkably, the detected thickness of immunocomplexes on the biochip surface can be further enhanced by up to 3 orders of magnitude if the secondary antibody is conjugated with magnetic nanoparticles (Orlov et al., 2015). Besides, the results of such magnetic nanolabel-based assays on passive multiplex biochips (Nikitin et al., 2018b) can be interrogated inductively by readers that employ nonlinear magnetization (Nikitin et al., 2018a; Orlov et al., 2016). Thus, many aspects of this development can be extended to other biosensing platforms, including those using conductive nanoparticles (Petryayeva and Krull, 2011; Cherkasov et al., 2020).

A substantial advantage of the developed multiplex biosensor is its flexibility for autoimmune disease diagnostics. To measure concentrations and/or kinetic characteristics of other autoantibody, the measuring setup will require minimal adaptation, namely, covalent immobilization of a respective antigen during preparation of the biochips and pumping the same antigen at the latest stage in analysis of kinetic characteristics. A possible limitation for the method extension to other autoantibodies can be relatively large antigen (comparable to IgG molecules). That is due to increased probability of binding of both Fab-fragments during sorption in the case of high-dense immobilization of low-molecular antigens. It is likely, however, that this issue can be resolved by optimization of the sorption density.

The biosensor design has virtually unlimited potential for multiplexing because of high compatibility with high-throughput microarray format on glass biochips, which permits simultaneous characterization of a large number of different autoantibodies. In addition, the quantification of concentration and aggressiveness of anti-TPO and anti-TG autoantibodies in combination with the previously reported ultrasensitive measuring of free thyroxine (LOD of 16 fg/mL) and thyroid stimulating hormone (LOD of 0.017 μIU/mL) in human serum (Znoyko et al., 2018, 2020) can be employed for advanced early diagnostics of thyroid diseases.

## 4. Conclusions

The advantages of presented label-free multiplex biosensor can be summarized as follows. This is the first tool that measures native kinetics of autoantibodies in serum. The native kinetics is measured with a free antigen as it behaves in blood (serum) rather than with an antigen sorbed on a surface as in tradition techniques. Additionally, concentration of autoantibody in serum can be measured with better sensitivity than that of the majority of label-based techniques and on par with that of the most sensitive chemiluminescence-based techniques. Both mentioned parameters can be registered simultaneously and independently during <25 min for various autoantibodies in different spots in the glass microarray format. The single-used biochips, which are microscope cover slips without additional thin film coatings, are widely available and cost-efficient. The disposable biochips are extremely important for routine medical screening for autoimmune disorders because autoantibodies should be measured directly in blood (serum), in which they are produced.

The native kinetics has been shown to be independent of concentration and promising as a novel criterion for differential diagnostics of autoimmune diseases.

The proposed biosensor is a promising tool for comprehensive clinical studies to elucidate eventually how the kinetic values of autoantibodies are associated with clinical symptoms in patients. The biosensor can be also extended to multiplex detection and kinetic characterization of other autoantibodies so that the pattern of concentration and kinetic parameters of a large number of autoantibodies can be employed for more accurate and early diagnostics. Besides, the developed method can be further adapted to other label-free sensors, for example, those based

on the surface plasmon resonance, optical waveguides, various types of interferometry, nanophotonic and mass sensitive structures, etc.

## CRediT author statement

*Alexey Orlov*: Conceptualization, Methodology, Validation, Formal analysis, Resources, Investigation, Data Curation, Writing – Original Draft, Writing – Review & Editing, Visualization, Project administration.

*Averyan Pushkarev*: Methodology, Validation, Formal analysis, Investigation, Data Curation, Writing – Original Draft, Writing – Review & Editing, Visualization.

*Sergey Znoyko*: Methodology, Investigation, Writing – Original Draft, Writing – Review & Editing, Visualization.

*Denis Novichikhin*: Methodology, Validation, Formal analysis, Investigation, Visualization.

*Vera Bragina*: Methodology, Formal analysis, Writing – Original Draft, Visualization, Funding acquisition.

*Boris Gorshkov*: Conceptualization, Methodology, Formal analysis, Data Curation, Writing – Review & Editing, Funding acquisition.

*Petr Nikitin*: Conceptualization, Methodology, Formal analysis, Resources, Writing – Original Draft, Writing – Review & Editing, Visualization, Supervision, Project administration, Funding acquisition.

## Declaration of competing interest

P.I.N. and B.G.G. are the named inventors on SCI-related patents.

## Acknowledgements

The authors are thankful to Evgeniya Kostrikina (Xema Medica, Russia) for her kind assistance in providing immunoreagents. A special word of gratitude is to Irina Nikitina (General Physics Institute, RAS, Russia) for the help with manuscript preparation and Dr. Svetlana Protasova (Resource Sharing Center, Institute of Solid State Physics, RAS, Russia) for registration of XPS-spectra. Different aspects and parts of this multidisciplinary research were partially supported by the grants of Russian Science Foundation #19-19-00716 (development of multiplex label-free interferometric biosensor and biochips), and #16-12-10543 (development of biosensing methods for rapid diagnosis, determination of their main analytical characteristics).

## References

Amos, M.D., Bridges, A.J., 2005. Standards for autoantibody testing; addressing future needs for autoimmune disease and cancer diagnosis. Canc. Biomarkers 1, 221–227.

Anderson, H., Jönsson, M., Vestling, L., Lindberg, U., Aastrup, T., 2007. Quartz crystal microbalance sensor design: I. Experimental study of sensor response and performance. Sensor. Actuator. B Chem. 123, 27–34.

ASCIA, 2013. Allergy and immune diseases in Australia (AIDA) report. February 2013. Available at: www.allergy.org.au/images/stories/reports/ASCIA_AIDA_Report_2013.pdf.

Ayela, C., Roquet, F., Valera, L., Granier, C., Nicu, L., Pugniere, M., 2007. Antibody–antigenic peptide interactions monitored by SPR and QCM-D: a model for SPR detection of IA-2 autoantibodies in human serum. Biosens. Bioelectron. 22, 3113–3119.

Božič, B., Čučnik, S., Kveder, T., Rozman, B., 2005. Avidity of anti-beta-2-glycoprotein I antibodies. Autoimmun. Rev. 4, 303–308.

Burenin, A.G., Urusov, A.E., Betin, A.V., Orlov, A.V., Nikitin, M.P., Ksenevich, T.I., Gorshkov, B.G., Zherdev, A.V., Dzantiev, B.B., Nikitin, P.I., 2015. Direct immunosensing by spectral correlation interferometry: assay characteristics versus antibody immobilization chemistry. Anal. Bioanal. Chem. 407, 3955–3964.

Campbell, C.T., Kim, G., 2007. SPR microscopy and its applications to high-throughput analyses of biomolecular binding events and their kinetics. Biomaterials 28, 2380–2392.

Campuzano, S., Pedrero, M., González-Cortés, A., Yáñez-Sedeño, P., Pingarrón, J.M., 2019. Electrochemical biosensors for autoantibodies in autoimmune and cancer diseases. Anal. Methods 11, 871–887.

Carlsson, J., Gullstrand, C., Westermark, G.T., Ludvigsson, J., Enander, K., Liedberg, B., 2008. An indirect competitive immunoassay for insulin autoantibodies based on surface plasmon resonance. Biosens. Bioelectron. 24, 876–881.

Chaloner-Larsson, G., Anderson, R., Egan, A., Da Fonseca Costa Filho, M.A., Gomez Herrera, J.F., Supply, V., 1999. A WHO Guide to Good Manufacturing Practice (GMP) Requirements.

Cherkasov, V.R., Mochalova, E.N., Babenyshev, A.V., Vasilyeva, A.V., Nikitin, P.I., Nikitin, M.P., 2020. Nanoparticle beacons: supersensitive smart materials with on/off-switchable affinity to biomedical targets. ACS Nano 14, 1792–1803.

Conigliaro, P., Chimenti, M.S., Triggianese, P., Sunzini, F., Novelli, L., Perricone, C., Perricone, R., 2016. Autoantibodies in inflammatory arthritis. Autoimmun. Rev. 15, 673–683.

Cooper, M.A., 2009. Label-free Biosensors: Techniques and Applications. Cambridge University Press.

Cui, Z., Zhao, M.-H., 2005. Avidity of anti-glomerular basement membrane autoantibodies was associated with disease severity. Clin. Immunol. 116, 77–82.

Damoiseaux, J., Andrade, L.E., Fritzler, M.J., Shoenfeld, Y., 2015. Autoantibodies 2015: from diagnostic biomarkers toward prediction, prognosis and prevention. Autoimmun. Rev. 14, 555–563.

Danczyk, R., Krieder, B., North, A., Webster, T., HogenEsch, H., Rundell, A., 2003. Comparison of antibody functionality using different immobilization methods. Biotechnol. Bioeng. 84, 215–223.

Drouvalakis, K.A., Bangsaruntip, S., Hueber, W., Kozar, L.G., Utz, P.J., Dai, H., 2008. Peptide-coated nanotube-based biosensor for the detection of disease-specific autoantibodies in human serum. Biosens. Bioelectron. 23, 1413–1421.

D'Aurizio, F., Metus, P., Ferrari, A., Caruso, B., Castello, R., Villalta, D., Steffan, A., Gaspardo, K., Pesente, F., Bizzaro, N., others, 2017. Definition of the upper reference limit for thyroglobulin antibodies according to the National Academy of Clinical Biochemistry guidelines: comparison of eleven different automated methods. Autoimmun. Highlights 8, 8.

Fan, X., White, I.M., Shopova, S.I., Zhu, H., Suter, J.D., Sun, Y., 2008. Sensitive optical biosensors for unlabeled targets: a review. Anal. Chim. Acta 620, 8–26.

Foo, K.Y., Hameed, B.H., 2010. Insights into the modeling of adsorption isotherm systems. Chem. Eng. J. 156, 2–10.

Fröhlich, E., Wahl, R., 2017. Thyroid autoimmunity: role of anti-thyroid antibodies in thyroid and extra-thyroidal diseases. Front. Immunol. 8, 521.

Hermanson, G.T., 2013. Chapter 2 – functional targets for bioconjugation. In: Hermanson, G.T. (Ed.), Bioconjugate Techniques. Academic Press, Boston.

Houen, G., 2019. Autoantibodies as diagnostic tools. In: Autoantibodies. Springer, pp. 1–11.

Ivanov, A.E., Solodukhina, N., Wahlgren, M., Nilsson, L., Vikhrov, A.A., Nikitin, M.P., Orlov, A.V., Nikitin, P.I., Kuzimenkova, M.V., Zubov, V.P., 2011. Reversible conformational transitions of a polymer brush containing boronic acid and its interaction with mucin glycoprotein. Macromol. Biosci. 11, 275–284.

Ivanov, A.E., Pushkarev, A.V., Orlov, A.V., Nikitin, M.P., Nikitin, P.I., 2019. Interferometric detection of chloramphenicol via its immunochemical recognition at polymer-coated nano-corrugated surfaces. Sensor. Actuator. B Chem. 282, 984–991.

Krumbholz, M., Derfuss, T., Hohlfeld, R., Meinl, E., 2012. B cells and antibodies in multiple sclerosis pathogenesis and therapy. Nat. Rev. Neurol. 8, 613.

Lleo, A., Invernizzi, P., Gao, B., Podda, M., Gershwin, M.E., 2010. Definition of human autoimmunity—autoantibodies versus autoimmune disease. Autoimmun. Rev. 9, A259–A266.

Mahler, M., Bentow, C., Serra, J., Fritzler, M.J., 2016. Detection of autoantibodies using chemiluminescence technologies. Immunopharmacol. Immunotoxicol. 38, 14–20.

Makaraviciute, A., Ramanaviciene, A., 2013. Site-directed antibody immobilization techniques for immunosensors. Biosens. Bioelectron. 50, 460–471.

Marrack, P., Kappler, J., Kotzin, B.L., 2001. Autoimmune disease: why and where it occurs. Nat. Med. 7, 899.

Martinez, O., Prabhakar, B.S., 2006. Autoantibodies in autoimmune thyroid disease. In: Pollard, K.M. (Ed.), Autoantibodies and Autoimmunity: Molecular Mechanisms in Health and Disease. Wiley-VCH Verlag GmbH & Co. KGaA, Weinheim.

Mauriz, E., Garcia-Fernández, M.C., Lechuga, L.M., 2016. Towards the design of universal immunosurfaces for SPR-based assays: a review. TrAC Trends Anal. Chem. 79, 191–198.

Mudumba, S., de Alba, S., Romero, R., Cherwien, C., Wu, A., Wang, J., Gleeson, M.A., Iqbal, M., Burlingame, R.W., 2017. Photonic ring resonance is a versatile platform for performing multiplex immunoassays in real time. J. Immunol. Methods 448, 34–43.

Nesterova, M., Johnson, N., Cheadle, C., Cho-Chung, Y.S., 2006. Autoantibody biomarker opens a new gateway for cancer diagnosis. Biochim. Biophys. Acta (BBA) - Mol. Basis Dis. 1762, 398–403.

Ngunjiri, J.N., Stark, D.J., Tian, T., Briggman, K.A., Garno, J.C., 2013. Immobilization of proteins on carboxylic acid functionalized nanopatterns. Anal. Bioanal. Chem. 405, 1985–1993.

Nikitin, P.I., Valeiko, M.V., Gorshkov, B.G., 2003. New direct optical biosensors for multi-analyte detection. Sensor. Actuator. B Chem. 90, 46–51.

Nikitin, P.I., Gorshkov, B.G., Nikitin, E.P., Ksenevich, T.I., 2005. Picoscope, a new label-free biosensor. Sensor. Actuator. B Chem. 111, 500–504.

Nikitin, M.P., Orlov, A.V., Sokolov, I.L., Minakov, A.A., Nikitin, P.I., Ding, J., Bader, S.D., Rozhkova, E.A., Novosad, V., 2018a. Ultrasensitive detection enabled by nonlinear magnetization of nanomagnetic labels. Nanoscale 10, 11642–11650.

Nikitin, M.P., Orlov, A.V., Znoyko, S.L., Bragina, V.A., Gorshkov, B.G., Ksenevich, T.I., Cherkasov, V.R., Nikitin, P.I., 2018b. Multiplex biosensing with highly sensitive magnetic nanoparticle quantification method. J. Magn. Magn Mater. 459, 260–264.

Orlov, A.V., Nikitin, M.P., Bragina, V.A., Znoyko, S.L., Zaikina, M.N., Ksenevich, T.I., Gorshkov, B.G., Nikitin, P.I., 2015. A new real-time method for investigation of affinity properties and binding kinetics of magnetic nanoparticles. J. Magn. Magn Mater. 350, 231–235.

Orlov, A.V., Bragina, V.A., Nikitin, M.P., Nikitin, P.I., 2016. Rapid dry-reagent immunomagnetic biosensing platform based on volumetric detection of nanoparticles on 3D structures. Biosens. Bioelectron. 79, 423–429.

Orlov, A.V., Pushkarev, A.V., Mochalova, E.N., Nikitin, P.I., Nikitin, M.P., 2018. Development and label-free investigation of logic-gating biolayers for smart biosensing. Sensor. Actuator. B Chem. 257, 971–979.
Petryayeva, E., Krull, U.J., 2011. Localized surface plasmon resonance: nanostructures, bioassays and biosensing—a review. Anal. Chim. Acta 706, 8–24.
Qiao, X., Zhang, X., Tian, Y., Meng, Y., 2016. Progresses on the theory and application of quartz crystal microbalance. Appl. Phys. Rev. 3, 31106.
Rose, N.R., 2008. Autoimmune diseases. In: International Encyclopedia of Public Health. Elsevier Inc., pp. 267–271
Rusmini, F., Zhong, Z., Feijen, J., 2007. Protein immobilization strategies for protein biochips. Biomacromolecules 8, 1775–1789.
Scarano, S., Mascini, M., Turner, A.P.F., Minunni, M., 2010. Surface plasmon resonance imaging for affinity-based biosensors. Biosens. Bioelectron. 25, 957–966.
Sciascia, S., Bertolaccini, M.L., 2016. Autoantibodies and biomarkers: diagnostic aspects. In: Connective Tissue Disease. Springer, pp. 47–59.
Scofield, R.H., 2004. Autoantibodies as predictors of disease. Lancet 363, 1544–1546.
Seydack, M., 2005. Nanoparticle labels in immunosensing using optical detection methods. Biosens. Bioelectron. 20, 2454–2469.
Su, X., Wu, Y.-J., Knoll, W., 2005. Comparison of surface plasmon resonance spectroscopy and quartz crystal microbalance techniques for studying DNA assembly and hybridization. Biosens. Bioelectron. 21, 719–726.
Thaler, M., Buhl, A., Welter, H., Schreiegg, A., Kehrel, M., Alber, B., Metzger, J., Luppa, P.B., 2009. Biosensor analyses of serum autoantibodies: application to antiphospholipid syndrome and systemic lupus erythematosus. Anal. Bioanal. Chem. 393, 1417–1429.
Thomsen, V., Schatzlein, D., Mercuro, D., 2003. Limits of detection in spectroscopy. Spectroscopy 18, 112–114.
Tozzoli, R., D'Aurizio, F., Ferrari, A., Castello, R., Metus, P., Caruso, B., Perosa, A.R., Sirianni, F., Stenner, E., Steffan, A., others, 2016. The upper reference limit for thyroid peroxidase autoantibodies is method-dependent: a collaborative study with biomedical industries. Clin. Chim. Acta 452, 61–65.
Tozzoli, R., Villalta, D., Bizzaro, N., 2017. Challenges in the standardization of autoantibody testing: a comprehensive review. Clin. Rev. Allergy Immunol. 53, 68–77.
Wu, J., Li, X., Song, W., Fang, Y., Yu, L., Liu, S., Churilov, L.P., Zhang, F., 2017. The roles and applications of autoantibodies in progression, diagnosis, treatment and prognosis of human malignant tumours. Autoimmun. Rev. 16, 1270–1281.
URL: https://www.isotop.hu http://www.izotop.hu/wordpress/pdf/immuno/rk8ct_a.pdf–. (Accessed 28 August 2019).
URL: https://www.isotop.hu http://www.izotop.hu/wordpress/pdf/immuno/rk36ct_a.pdf–. (Accessed 28 August 2019).
Zhang, J., Zhao, J., 2018. Immuno-Biosensor, Nano-Inspired Biosensors for Protein Assay with Clinical Applications. Elsevier Inc.
Znoyko, S.L., Orlov, A.V., Bragina, V.A., Nikitin, M.P., Nikitin, P.I., 2020. Nanomagnetic lateral flow assay for high-precision quantification of diagnostically relevant concentrations of serum TSH. Talanta 216, 120961.
Znoyko, S.L., Orlov, A.V., Pushkarev, A.V., Mochalova, E.N., Guteneva, N.V., Lunin, A.V., Nikitin, M.P., Nikitin, P.I., 2018. Ultrasensitive quantitative detection of small molecules with rapid lateral-flow assay based on high-affinity bifunctional ligand and magnetic nanolabels. Anal. Chim. Acta 1034, 161–167.